

The Role of Tetrahydrobiopterin in the Regulation of Neuronal Nitric-oxide Synthase-generated Superoxide*

Received for publication, January 28, 2002, and in revised form, August 13, 2002
Published, JBC Papers in Press, August 14, 2002, DOI 10.1074/jbc.M200853200

Gerald M. Rosen^{‡§¶}, Pei Tsai[‡], John Weaver[¶], Supatra Porasuphatana^{**}, Linda J. Roman^{‡‡}, Anatoly A. Starkov^{§§}, Gary Fiskum^{§§}, and Sovitj Pou[‡]

From the [‡]Department of Pharmaceutical Sciences, University of Maryland School of Pharmacy, Baltimore, Maryland 21201 and the Medical Biotechnology Center, University of Maryland Biotechnology Institute, Baltimore, Maryland 21201, the [§]Center for Low Frequency EPR for in Vivo Physiology, University of Maryland School of Pharmacy, Baltimore, Maryland 21201, the [¶]Department of Chemistry, University of Maryland Baltimore County, Baltimore, Maryland 21250, the ^{**}Department of Toxicology, Faculty of Pharmaceutical Science, Khon Kaen University, Khon Kaen 40002, Thailand, the ^{‡‡}Department of Biochemistry, The University of Texas Health Science Center, San Antonio, Texas 78229, and the ^{§§}Department of Anesthesiology, University of Maryland School of Medicine, Baltimore, Maryland 21201

Tetrahydrobiopterin (H₄B) is a critical element in the nitric-oxide synthase (NOS) metabolism of L-arginine to L-citrulline and NO[•]. It has been hypothesized that in the absence of or under nonsaturating levels of L-arginine where O₂ reduction is the primary outcome of NOS activation, H₄B promotes the generation of H₂O₂ at the expense of O₂^{•−}. The experiments were designed to test this hypothesis. To test this theory, two different enzyme preparations, H₄B-bound NOS I and H₄B-free NOS I, were used. Initial rates of NADPH turnover and O₂ utilization were found to be considerably greater in the H₄B-bound NOS I preparation than in the H₄B-free NOS I preparation. In contrast, the initial generation of O₂^{•−} from the H₄B-free NOS I preparation was found to be substantially greater than that measured using the H₄B-bound NOS I preparation. Finally, by spin trapping nearly all of the NOS I produced O₂^{•−}, we found that the initial rate of H₂O₂ production by H₄B-bound NOS I was considerably greater than that for H₄B-free NOS I.

Neuronal nitric-oxide synthase (NOS I),¹ a member of a family of heme-containing monooxygenases that metabolize L-arginine to NO[•] and L-citrulline (1, 2), contains an N-terminal oxidase domain with binding sites for L-arginine and (6R)-5,6,7,8-tetrahydro-L-biopterin (H₄B) and a C-terminal reductase domain with binding sites for FMN, FAD, and NADPH. The domains are connected by a Ca²⁺/calmodulin-binding region that allows electron transport through the enzyme (3). One rather interesting finding is that H₄B, although not essential for heme reduction (4), is nevertheless necessary for significant production of NO[•] from L-arginine (5). This co-factor stabilizes the dimeric structure of NOS (6–8), enhances substrate affinity (9, 10), increases the rate of NADPH consumption (4,

11), promotes destabilization of the NOS-Fe²⁺O₂ species (12), and regulates the mid-point potential of NOS heme (4).

In 1992, we discovered that NOS I generates O₂^{•−} in the absence of L-arginine (13). More recently, NOS II and NOS III, like NOS I, have been found to generate O₂^{•−} during enzymic cycling (14–16). In the presence of L-arginine, NOS I generates NO[•] and O₂^{•−}; the ratio of these free radicals is dependent upon the concentration of L-arginine (17, 18). Thus, L-arginine is one of the controlling factors that dictate the selectivity of free radicals produced by NOS. However, in the absence of substrate, NOS uses O₂ as the terminal electron acceptor, generating O₂^{•−} and H₂O₂ by sequential one-electron reductive steps (see Fig. 1). Under these conditions, there is undoubtedly an alternative mechanism by which NOS regulates the formation of each of these cell-signaling products of O₂ reduction. One possibility is that H₄B controls production of O₂^{•−} by increasing the reduction rate of the NOS-Fe²⁺O₂ species (Refs. 19–22 and Fig. 1). Evidence to support this theory comes from experiments where the addition of H₄B to purified NOS I diminished the spin trapping of O₂^{•−} (17, 18, 23). However, these findings must be viewed with caution, because H₄B in aqueous solution has been reported to scavenge O₂^{•−} (24–26) with a rate constant of 3.9 × 10⁵ M^{−1} s^{−1} (26). Thus, the conclusion drawn from the earlier studies (17, 18, 23) that H₄B regulates NOS production of O₂^{•−} is unsubstantiated, because free H₄B and the spin trap compete for NOS-produced O₂^{•−} (26). In contrast, when H₄B is bound to NOS at the heme near the dimer interface (27, 28), this pterin is thought not to undergo such reactions. This paper describes a series of experiments designed to test whether H₄B bound to NOS is pivotal in shifting the rate of electron flow to the NOS-Fe²⁺O₂ species, thereby promoting formation of H₂O₂ at the expense of O₂^{•−}.

EXPERIMENTAL PROCEDURES

Materials—NADPH, calmodulin, L-arginine, calcium chloride, H₂O₂, and horseradish peroxidase were purchased from Sigma-Aldrich. Superoxide dismutase was obtained from Roche Diagnostics (Mannheim, Germany). H₄B was obtained from Schircks Laboratories (Jona, Switzerland). L-[U-¹⁴C]Arginine monohydrochloride ([¹⁴C]L-arginine) was purchased from Amersham Biosciences. Dowex® 50W-X8 cation exchange resin was obtained from Bio-Rad. Amplex Red (10-acetyl-3,7-dihydroxyphenoxazine) was purchased from Molecular Probes (Portland, OR). Amplex Red was dissolved in Me₂SO and stored under N₂ at −80 °C until use. The spin trap for O₂^{•−}, 5-tert-butoxycarbonyl-5-methyl-1-pyrroline N-oxide (BMPO) was prepared according to the method described by Zhao *et al.* (29). All other chemicals were used as purchased without further purification.

Purification of NOS I—NOS I was expressed and purified essentially as described by Roman *et al.* (30), with the modification that the culture

* This work was supported in part by National Institutes of Health Grants RR-12257 (to G. M. R.), T32-ES07263 (to P. T.), R25-GM-55036 (to J. W.), NS-34152 (to G. F.), and GM-52419 and Robert A. Welch Foundation Grant AQ1192. The costs of publication of this article were defrayed in part by the payment of page charges. This article must therefore be hereby marked "advertisement" in accordance with 18 U.S.C. Section 1734 solely to indicate this fact.

¶ To whom correspondence should be addressed: Univ. of Maryland School of Pharmacy, 725 West Lombard St., Baltimore, MD 21201. Tel.: 410-706-0514; Fax: 410-706-8184; E-mail: grosen@umaryland.edu.

¹ The abbreviations used are: NOS, nitric-oxide synthase; H₄B, (6R)-5,6,7,8-tetrahydro-L-biopterin; BMPO, 5-tert-butoxycarbonyl-5-methyl-1-pyrroline N-oxide; SOD, superoxide dismutase; HRP, horseradish peroxidase; DEPMPPO, 5-(diethoxyphosphoryl)-5-methyl-1-pyrroline-N-oxide; DMPO, 5,5-dimethyl-1-pyrroline-N-oxide.

volume was 500 ml rather than 1000 ml. The effluent from the ADP-Sepharose column was divided into two fractions: one that was reconstituted with H₄B (250 μM) at 4 °C and one that was not. Neither fraction was exposed to L-arginine at any point during purification. After overnight incubation on ice, both of the fractions were applied to an S-200 gel filtration column (Pharmacia Corp.) to remove excess H₄B and to further purify the enzyme. The dimer peak was collected and concentrated. The enzyme concentration was determined by its CO difference spectrum, as described in Ref. 30, using an extinction coefficient of 100 mM⁻¹ cm⁻¹ at Δε 444–475 nm. Neither fraction was ever frozen but was stored on ice and used the next day.

NADPH Consumption—Oxidation of NADPH was performed in a reaction using potassium phosphate buffer (50 mM, pH 7.4, 1 mM DTPA, 1 mM EGTA), CaCl₂ (2 mM), calmodulin (100 units/ml), and NADPH (150 μM) at room temperature. The reaction was initiated by the addition of NOS I (0.40 μM). A UV-visible spectrophotometer (Uvikon, model 940, Research Instruments International, San Diego, CA) was used to monitor the reaction spectrophotometrically at 340 nm. The initial rate of NADPH oxidation was estimated using an extinction coefficient of 6.22 mM⁻¹ cm⁻¹.

Oxygen Consumption—Oxygen consumption was measured with a commercial oxygen monitoring system (Hansatech). The system was composed of a membrane-coated Clark-type electrode fitted in a glass body reaction chamber and equipped with a Teflon-coated stirring bar and an air-tight stopper. Data acquisition was performed with proprietary hardware and software (Hansatech). All of the measurements were performed at 25 °C. In a typical experiment, NADPH (150 μM) was added to either a solution of H₄B-bound NOS I (0.40 μM) or H₄B-free NOS I (0.40 μM). The initial rate of O₂ consumption was measured, assuming an initial O₂ concentration equal to 253.4 nmol/ml (31).

Spin Trapping Superoxide from NOS—Spin trapping of O₂⁻ from purified H₄B-free NOS I and H₄B-bound NOS I was conducted by mixing all components described in the text to a final volume of 0.25 ml. The reaction mixture was then transferred to a flat quartz cell and placed into the cavity of an EPR spectrometer (model E-109; Varian Medical Systems, Inc., Palo Alto, CA). The EPR cell was open to the air, allowing O₂ to enter the quartz cell. EPR spectra were recorded at room temperature. Instrument settings were: microwave power, 20 mW; modulation frequency, 100 kHz; modulation amplitude, 0.5 G; sweep time, 12.5 G/min; and response time, 0.5 s. The receiver gain is given in the legend to Fig. 2.

Rate of Spin Trapping of Superoxide—The apparent rate constant for the spin trapping of O₂⁻ by BMPO, generating the corresponding spin-trapped adduct of O₂⁻, BMPO-OOH, was estimated using the model O₂⁻ generating system of xanthine/xanthine oxidase. The reaction mixture contained BMPO (60 mM), hypoxanthine (400 μM), and sufficient xanthine oxidase to generate 1 μM/min of O₂⁻ as determined by the SOD-inhibitable reduction of ferricytochrome *c* (80 μM) at 550 nm using an extinction coefficient of 21 mM⁻¹ cm⁻¹ (32).

Ferricytochrome *c* (0–23 μM) was used as a competitive inhibitor (33). The reaction mixtures were immediately transferred to an EPR flat quartz cell and introduced into the cavity of the EPR spectrometer (model E-109; Varian Medical Systems, Inc.). EPR spectra were recorded at room temperature 3 min after the reaction was initiated by the addition of xanthine oxidase. Instrument settings were: microwave power, 20 mW; modulation frequency, 100 kHz; modulation amplitude, 0.5 G; sweep time, 12.5 G/min; and response time, 0.5 s.

Estimation of the Half-life of BMPO-OOH—The half-life of BMPO-OOH was determined by monitoring the decrease in the first line of the EPR spectrum of BMPO-OOH as a function of time. The reaction mixture contained BMPO (50 mM) and hypoxanthine (400 μM) in potassium phosphate buffer (chelexed, 50 mM, pH 7.4, 1 mM DTPA) for 10 min, and then SOD (30 units/ml, as defined in Ref. 34) was added. The reaction mixture was immediately transferred to an EPR flat quartz cell and introduced into the cavity of the EPR spectrometer (model E-109; Varian Medical Systems, Inc.). EPR spectra were recorded at various time intervals for 60 min.

Rate of Hydrogen Peroxide Formation—Estimation of H₂O₂ production was obtained by fluorometric analyses (fluorometer, Hitachi model F2500, High Technologies America, Inc., San Jose, CA). A modified method utilizing the dye Amplex Red was adopted (35–37). The incubation medium was supplemented with Amplex Red (1 μM) and horseradish peroxidase (5 units/ml) in sodium phosphate buffer (50 mM, 1 mM EGTA, pH 7.4). The reaction mixture contained NADPH (160 μM), CaCl₂ (0.5 mM), calmodulin (100 units/ml), BMPO (100 mM), and SOD (0.04–80 units/ml). SOD (0.04 unit/ml) was added to each reaction to suppress initial fluorescence seen from the inclusion of NADPH, and SOD (0.14–80 units/ml) was used in control experiments described

under “Results and Discussion.” The reaction was initiated by the addition of purified H₄B-free NOS I (4 nM) or H₄B-bound NOS I (4 nM) into the reaction mixture. The initial rate of H₂O₂ generation was recorded as an increase in fluorescence of the dye at 585 nm with the excitation set at 550 nm. The fluorescence was calibrated by generating a standard curve with known concentrations of H₂O₂. The concentration of the commercial 30% H₂O₂ solution was calculated from light absorbance at 240 nm employing an extinction coefficient of 0.0436 mM⁻¹ cm⁻¹; the stock solution was diluted to 50 μM with water and used for calibration immediately. The specificity of horseradish peroxidase/Amplex Red toward H₂O₂ was confirmed, because *tert*-butyl hydroperoxide was not found to be a substrate.

NOS I Activity by [¹⁴C]-L-Citrulline Formation Assay—The enzymatic activity of purified NOS I was determined by its ability to catalyze the formation of L-citrulline from L-arginine as previously reported (17) with modifications. The reaction mixture contained purified NOS I (0.15 μM), CaCl₂ (2 mM), and mixture solution ([¹⁴C]-L-arginine (0.6 μCi/ml) in the presence of NADPH (1 mM), L-arginine (50 μM), and calmodulin (100 units/ml) in HEPES buffer (50 mM HEPES, 0.5 mM EGTA, pH 7.4). The reaction was initiated by the addition of the mixture solution into the reaction mixture containing purified NOS I and CaCl₂ in the presence of various concentrations of BMPO ranging from 50 to 150 mM. The reaction mixture was incubated at 23 °C for 10 min and terminated with 2 ml of stop solution (20 mM HEPES, 2 mM EDTA, pH 5.5). The product [¹⁴C]-L-citrulline was separated by passing the reaction mixture through columns containing Dowex® 50W-X8 cation exchange resin preactivated with a NaOH solution (1 M), and radioactivity was counted using a scintillation counter (model LS 6500; Beckman Coulter Inc., Fullerton, CA).

RESULTS AND DISCUSSION

In the absence of L-arginine, NOS I generates O₂⁻ and H₂O₂; the latter was from either self-dismutation from O₂⁻ or direct enzymic formation of H₂O₂. These reduction products of O₂ mediate different cell signaling pathways. Thus, it is important to understand how NOS I regulates formation of O₂⁻ and H₂O₂. Clearly, one controlling factor is L-arginine, which upon oxidation by NOS to L-citrulline and NO[•] decreases the production of O₂⁻ (13, 18, 23). Another limiting factor may be H₄B, because this pterin appears to be a critical element in shifting the competition between O₂⁻ generation and direct production of H₂O₂. Here, the experiments are aimed at testing this hypothesis.

As a source of NOS I, we used recombinant enzyme expressed in *Escherichia coli*. When isolated from this bacterium, NOS does not contain H₄B. For these studies, H₄B (250 μM) was added to a portion of the isolated NOS and incubated overnight at 4 °C, and this mixture was subsequently passed through an S-200 gel filtration column to remove excess H₄B. Nitric-oxide synthase I isolated in this manner is complemented with about 0.65 nmol H₄B/nmol enzyme, *i.e.* 65% saturated (30). No excess, unbound H₄B is present. With these two preparations, H₄B-free NOS I and H₄B-bound NOS I, we investigated whether H₄B regulates O₂⁻ generation.

In our first series of experiments, we estimated the initial rate of NADPH oxidation by incubating NADPH (150 μM) with either H₄B-free NOS I (0.40 μM) or H₄B-bound NOS I (0.40 μM) and CaCl₂ (2 mM)/calmodulin (100 units/ml). These are important rates to measure, because both enzyme preparations generate O₂⁻ in the absence of L-arginine. Thus, the flux of O₂⁻ and the direct enzymic formation of H₂O₂ from H₄B-free NOS and H₄B-bound NOS is dependent on the initial rate of NADPH turnover. We found that the initial rate of NADPH oxidation with H₄B-bound NOS I was 164 ± 24 nmol/min/mg protein, whereas with H₄B-free NOS I, the initial rate of NADPH consumed was 59 ± 7 nmol/min/mg protein. This enhanced rate of NADPH oxidation when H₄B is bound to NOS I was similar to that previously reported (11).

In the absence of L-arginine, the final electron acceptor from the NADPH/NOS reduction is O₂, yielding O₂⁻ and H₂O₂. Hydrogen peroxide can arise from the dismutation of O₂⁻ as well as the one-electron reduction of NOS-Fe²⁺O₂ followed by release

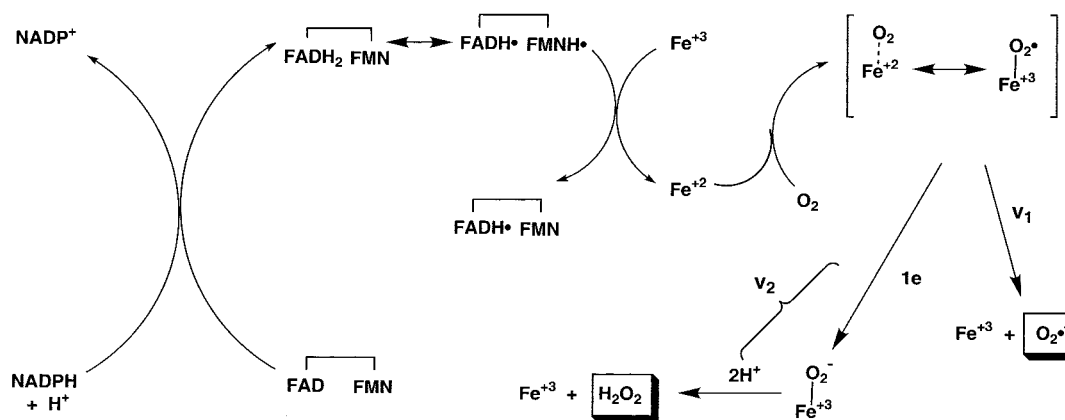
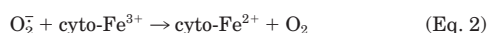


FIG. 1. A model depicting the formation of O_2^- and H_2O_2 by NOS I in the absence of L-arginine. We envision that $[Fe^{3+}-O_2]$ releases O_2^- with a rate v_1 that in the case of H_4B -free NOS is considerably faster than H_4B -bound NOS. When H_4B bound to NOS, $[Fe^{3+}-O_2]$ is reduced with a rate v_2 that results in enhanced production of H_2O_2 at the expense of O_2^- .

of H_2O_2 (Fig. 1). Not surprisingly, according to O_2 consumption experiments, we found that independent of the NOS preparation, 1 mol of NADPH oxidized resulted in 1 mol of O_2 consumed (data not shown); the difference is in the ratio of the initial O_2 reduction products. The experiments were then designed to determine the onset of O_2^- production and the initial rate of H_2O_2 formation from H_4B -free NOS I and H_4B -bound NOS I.

We first explored the production of O_2^- by both enzyme preparations. For the detection of O_2^- , we used spin trapping and EPR spectroscopy as alternative methods to determine whether NOS-derived O_2^- are artifact prone (13). For instance, we have previously demonstrated that NOS I will reduce ferricytochrome *c* at a rate faster than its reaction with O_2^- (13). For these experiments, the nitron BMPO was used because recent publications (29, 38) suggested that this compound is the best of the next generation of spin traps for O_2^- . Surprisingly, the rate constant for the reaction of BMPO with O_2^- was not calculated (29). Because this is an important factor in assessing the efficiency of spin trapping O_2^- , this constant was determined.

An apparent rate constant for spin trapping O_2^- by BMPO was estimated using ferricytochrome *c* as a competitive inhibitor (33), because the rate constant for its reaction with O_2^- is known (39). Further, ferricytochrome *c* does not interfere with the EPR spectrum of BMPO-OOH. The reaction of BMPO and ferricytochrome *c* with O_2^- can be expressed as follows.



From Equations 1 and 2, the rate of O_2^- elimination in the presence of ferricytochrome *c* can be represented as follows.

$$-d[O_2^-]/dt = k_{\text{app}}[\text{BMPO}][O_2^-] + k_{\text{cyto-Fe}^{2+}}[\text{cyto-Fe}^{3+}][O_2^-] \quad (\text{Eq. 3})$$

In the absence of cytochrome *c*, Equation 3 can be described as follows.

$$d[\text{BMPO-OOH}]/dt = k_{\text{app}}[\text{BMPO}][O_2^-] \quad (\text{Eq. 4})$$

By dividing Equation 4 into Equation 3 and rearranging the terms, the competing reactions become the following.

$$\begin{aligned} d[O_2^-]/dt / (d[\text{BMPO-OOH}]/dt) \\ = 1 + k_{\text{cyto-Fe}^{2+}}[\text{cyto-Fe}^{3+}] / k_{\text{app}}[\text{BMPO}] \quad (\text{Eq. 5}) \end{aligned}$$

Under our experimental conditions, the concentration of BMPO is in great excess with respect to the concentration of O_2^- .

Therefore, the relative concentration of the spin-trapped adduct, as determined by EPR spectral peak height, is directly related to k_{app} and $k_{\text{cyto-Fe}^{2+}}$, the rate constants for the spin trapping of O_2^- by BMPO and ferricytochrome *c*, respectively, at a given concentration of BMPO. Thus, Equation 5 can be represented as follows.

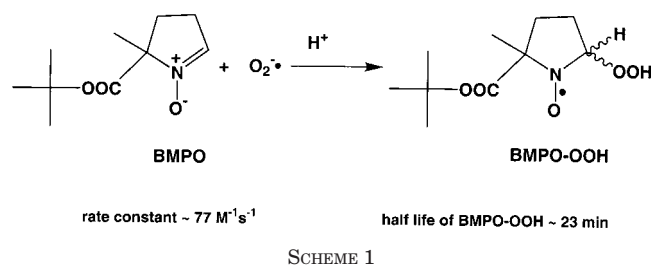
$$A_0/A = 1 + k_{\text{cyto-Fe}^{2+}}[\text{cyto-Fe}^{3+}] / k_{\text{app}}[\text{BMPO}] \quad (\text{Eq. 6})$$

where A_0 and A represent the rate of spin trapping O_2^- (EPR spectral peak height) in the absence and presence of ferricytochrome *c*, respectively (33). If the concentration of the BMPO is fixed, then a plot of A_0/A versus $[\text{cyto-Fe}^{3+}]$ generates a straight line, and the slope is $k_{\text{cyto-Fe}^{2+}}/k_{\text{app}}[\text{BMPO}]$ (40). By using the known rate constant for the reduction of ferricytochrome *c* by O_2^- to ferrocyanochrome *c*, $k_{\text{cyto-Fe}^{2+}} = 1.1 \times 10^6 \text{ M}^{-1} \text{ s}^{-1}$ (39), the k_{app} for BMPO can be calculated. We found $k_{\text{app}} = 77 \pm 5 \text{ M}^{-1} \text{ s}^{-1}$ ($n = 6$).

We then determined the stability of BMPO-OOH. For these experiments, xanthine/xanthine oxidase was used as a continuous source of O_2^- , which in these studies afforded a low flux of $1 \mu\text{M } O_2^-/\text{min}$. After 10 min, SOD (30 units/ml) was added to quench the reaction. We found the half-life of BMPO-OOH to be $22.8 \pm 0.9 \text{ min}$ ($n = 6$) at pH 7.4 (Scheme 1).

In choosing the best spin trap to estimate O_2^- production from both enzyme preparations, we need a nitron whose corresponding spin-trapped adduct of O_2^- displays an EPR spectrum that is sufficiently robust to allow accurate measurements of spectral peak heights as a function of time. It appears that BMPO is the appropriate spin trap for these studies. We arrive at this decision based on three important findings. First, the rate constant for the reaction of BMPO with O_2^- exceeded that of DMPO, which had been reported to be $15 \text{ M}^{-1} \text{ s}^{-1}$ (41), and it was slightly slower than that found for DEPMPPO at $90 \text{ M}^{-1} \text{ s}^{-1}$ (42). Second, the half-life of BMPO-OOH was considerably greater than for that of DMPO-OOH at 53 s (43) and in the same range as that for DEPMPPO-OOH at 18 min (44). Third, the EPR spectrum of BMPO-OOH exhibited a greater signal-to-noise ratio than that found for DEPMPPO-OOH. The small signal-to-noise ratio of DEPMPPO-OOH was the result of additional hyperfine splitting associated with the phosphorous atom located at the α -carbon on the pyrroline ring.

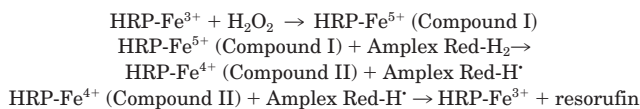
Next, we explored the difference in O_2^- production from H_4B -bound NOS I and H_4B -free NOS I. For these experiments, BMPO (50 mM) was added to a solution containing either H_4B -bound NOS I (0.31 μM) or H_4B -free NOS I (0.31 μM), NADPH (1 mM), and CaCl_2 (2 mM)/calmodulin (100 units/ml). We estimated the rate of producing O_2^- by measuring the low field EPR



spectral peak height as a function of time (see *inset* in Fig. 2). Fig. 2 reveals several novel findings. First, H₄B-bound NOS I and H₄B-free NOS I generated O₂⁻ in the absence of L-arginine. Second, at early time points, within the first several min after the reaction had commenced, H₄B-free NOS I produced more O₂⁻ than that found for H₄B-bound NOS. This result is remarkable when one considers that the turnover rate for H₄B-bound NOS is 2.8 times faster than that for H₄B-free NOS. Over time, the difference in the EPR spectral peak heights of BMPO-OOH from H₄B-free NOS I and H₄B-bound NOS I disappeared, approaching equality after only 4–5 min. When equilibrium had been reached, at ~ 8 min, the amount of O₂⁻ spin-trapped by BMPO from H₄B-bound NOS I had far exceeded that from H₄B-free NOS I.

We then investigated the source of H₂O₂ from H₄B-bound NOS and H₄B-free NOS. Hydrogen peroxide can be generated from the one-electron reduction of the NOS-Fe²⁺O₂ species followed by release of H₂O₂ (Fig. 1). Alternatively, this peroxide can arise from the dismutation of O₂⁻, in which the rate constant at pH 7.4 is $3.0 \times 10^5 \text{ M}^{-1} \text{ s}^{-1}$ (45). It is therefore by no means a trivial task to separate these disparate pathways. After considering several options, we settled on an approach that required increasing the concentration of BMPO to a level so that this nitroxide would spin trap most, if not all, of the O₂⁻ produced (41). Thereupon, the only source of NOS-derived H₂O₂ would be from the one-electron reduction of the NOS-Fe²⁺O₂ species.

We then had to find a method that would meet the following criteria. First, the assay had to detect H₂O₂ in real time, not at some arbitrary time after the reaction had commenced. Second, the method must not interfere with the spin trapping of O₂⁻. Third, given that NOS can easily transfer electrons to a wide variety of one-electron acceptors, such as ferricytochrome *c* (13), the assay had to be an oxidative process. Fourth, the method had to be sensitive and selective for H₂O₂. Given these limitations, we settled on a fluorometric assay developed by Zhou *et al.* (36, 37). The overall mechanism, shown below, involves three distinct reactions, as presented by Chance (46). In the first step, H₂O₂ is reduced by horseradish peroxidase to Compound I. In the second step, Amplex Red is then oxidized by Compound I to give Compound II and the Amplex Red free radical intermediate. This intermediate then reacts with Compound II to regenerate horseradish peroxidase and the corresponding quinone, resorufin, which is the source of the fluorescent measurement (35–37).



REACTIONS 1–3

Although the rate constant for the reaction of H₂O₂ with horseradish peroxidase to form Compound I is $10 \times 10^6 \text{ M}^{-1} \text{ s}^{-1}$ (46), the rate constants for the sequential one-electron reduction of Compounds I and II to the fluorescent resorufin from Amplex Red are unknown. However, based on similar reactions reported in the literature (46) involving Compound I and II

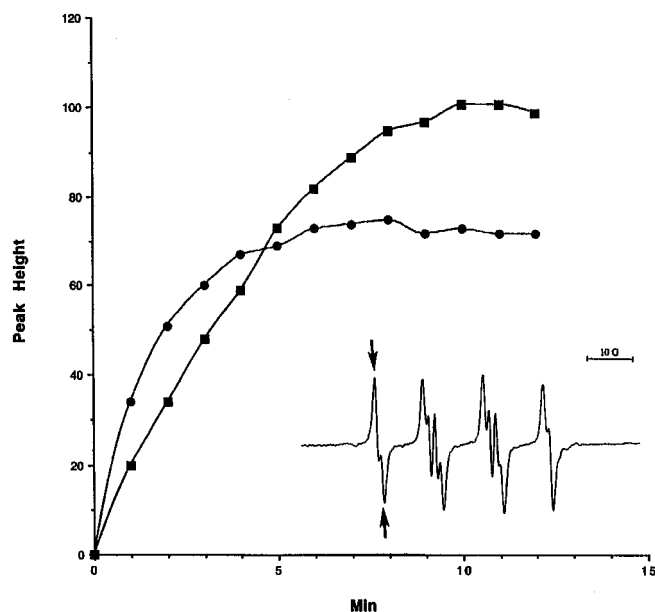


FIG. 2. A representative plot of the increase in the first low field peak (arrows in the *inset*) of EPR spectrum of BMPO-OOH. This nitroxide is derived from the reaction of O₂⁻ with BMPO as a function of time. ●, EPR spectral data of BMPO-OOH from the spin trapping of H₄B-free NOS I generated O₂⁻. ■, EPR spectral data of BMPO-OOH from the spin trapping of H₄B-bound NOS I generated O₂⁻. *Inset*, the EPR spectrum of BMPO-OOH was obtained 8 min after the spin trapping of O₂⁻ by H₄B-bound NOS I. The hyperfine splitting constants for BMPO-OOH are the same as those reported in the literature (29) and are $A_N = 13.4$ and $A_H = 12.0$ for one isomer and $A_N = 13.4$ and $A_H = 9.4$ for the other isomer. The receiver gain is 2×10^4 .

with other donor molecules, we estimate that the rate constant would not be above $1 \times 10^5 \text{ M}^{-1} \text{ s}^{-1}$, and most likely it is close to $1 \times 10^3 \text{ M}^{-1} \text{ s}^{-1}$, too slow to allow quantitative estimates of the initial rate of H₂O₂ production. Therefore, the initial rate of NADPH consumption measured does not have a direct 1:1 relationship with the initial rate of H₂O₂ generated, as estimated by this fluorescent technique. Rather, only the ratio of initial rates of H₂O₂ formation can be used to draw conclusions about the relative fluxes of direct H₂O₂ generated by H₄B-bound NOS and H₄B-free NOS preparations.

Before we could measure the rate of H₂O₂ production from H₄B-bound NOS I and H₄B-free NOS I, however, a series of control experiments were conducted. Initially, we determined the appropriate concentration of BMPO for the fluorescent assay. Our goal was to find a concentration of BMPO that would maximally spin trap O₂⁻ without inhibiting NOS. For these studies, we added NADPH (1 mM) and CaCl₂ (2 mM)/calmodulin (100 units/ml) to H₄B-bound NOS I (0.40 μM) while we varied the concentration of BMPO from 50 to 150 mM. We found that at BMPO concentrations above 125 mM, there was no increase in the EPR spectral peak height of BMPO-OOH (data not shown). Under identical experimental conditions, NOS I activity was assessed by determining what effect, if any, BMPO had on enzymatic activity. We incubated NADPH (1 mM), CaCl₂ (2 mM)/calmodulin (100 units/ml), L-arginine (50 μM), [¹⁴C]L-arginine (0.6 $\mu\text{Ci/ml}$) with H₄B-bound NOS I (0.15 μM), and BMPO (ranging from 0 to 150 mM). At concentrations of BMPO greater than 100 mM, significant inhibition in NOS activity was observed. Therefore, we chose a concentration of BMPO at 100 mM for the fluorescent experiments.

Next, we determined the effectiveness of BMPO (100 mM) to compete with SOD for NOS-derived O₂⁻ in the fluorescent assay. For these experiments, we mixed NADPH (160 μM) with H₄B-bound NOS I (57 nM), CaCl₂ (500 μM)/calmodulin (100 units/

ml), and SOD (ranging from 0.14 to 80 units/ml). We found that the rate of H_2O_2 production, as measured by an increase in fluorescence, was constant over this range of SOD used in the experiment (data not shown). Thus, where appropriate SOD (0.14 units/ml) was included in each reaction. When BMPO (100 mM) was added to the above reaction mixture, without and with SOD (0.14 units/ml), we found that BMPO spin-trapped $\sim 90\%$ of the O_2^- generated by NOS.

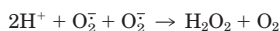
Based on these control experiments, we were confident that by inclusion of BMPO in the reaction mixture, most of the NOS-produced O_2^- was spin-trapped. It is important to reiterate that although this fluorometric assay is very sensitive and selective for H_2O_2 , the efficiency of this method is unknown. Nevertheless, when the reaction was conducted using only 4 nM of H_4B -bound NOS I and H_4B -free NOS I, we obtained an initial rate of H_2O_2 formation of 28.7 ± 8.6 and 12.5 ± 2.5 nmol/min/mg protein, respectively.

CONCLUSION

The experiments presented here were designed to examine whether H_4B , bound to NOS I, regulates O_2^- production. In previous studies (17, 18, 23), H_4B was added to a NOS I preparation. The observed diminished spin trapping of O_2^- may have been the result of excess H_4B , which may not have been bound to NOS, that scavenged O_2^- . In the experiments conducted, unbound H_4B was removed by passing the H_4B -containing NOS I preparation through a gel filtration column, isolating only H_4B -bound NOS I.

The data presented here support our hypothesis that bound H_4B promoted the direct formation of H_2O_2 at the expense of O_2^- production. Once the heme- O_2 intermediate NOS-(Fe^{3+})(O_2) is formed, it can either release O_2^- with a rate v_1 or accept an electron, forming NOS-(Fe^{3+})(O_2^-), which subsequently releases H_2O_2 with an overall rate v_2 (Fig. 1). Our findings demonstrate that activated NOS generated O_2^- , whether or not the enzyme contained bound H_4B . At early time points, O_2^- released from NOS was considerably less when H_4B was bound to the enzyme than in the absence of this pterin (Fig. 2). After several min, however, the EPR spectral peak height of BMPO-OOH (Scheme 1) from H_4B -bound NOS I out-paced that observed with H_4B -free NOS I (Fig. 2). This observation demonstrates that H_4B -bound NOS I generated more O_2^- during the length of the experiments, even though the initial production of O_2^- was greater with H_4B -free NOS I (Fig. 2). This finding was expected, because the turnover rate for H_4B -bound NOS I was nearly 2.8 times greater than that for H_4B -free NOS I.

By increasing the concentration of BMPO to 100 mM and decreasing the concentration of NOS from 57 to 4 nM, we estimate that BMPO spin-trapped $\sim 90\%$ of the O_2^- generated from NOS, independent of whether H_4B was bound to the enzyme. Thus, we were able to use a fluorescent technique that appears to be sensitive and specific for H_2O_2 to distinguish between differing sources of H_2O_2 , as the decomposition of NOS-(Fe^{3+})(O_2^-) and the self-dismutation of O_2^- contribute to the general pool of H_2O_2 .



REACTION 4

Our findings point to the fact that NADPH/ H_4B -bound NOS I yielded considerably more H_2O_2 than did NADPH/ H_4B -free NOS I, even though both enzyme preparations reduce O_2 to O_2^- . Given that NOS secretes O_2^- and H_2O_2 , measuring H_2O_2 without eliminating O_2^- will undoubtedly lead to an overestimation of the direct NOS produced H_2O_2 . It is worth noting that to our knowledge, this is the first report that unequivocally demonstrates that NOS I independently generates both O_2^- and H_2O_2 .

Finally, it is important to point out that H_4B plays a dual role in NOS reduction in the absence of L-arginine. First, this pterin enhances the rate of NADPH turnover. Second H_4B shifts the ratio of O_2 reduction products by increasing the rate of direct H_2O_2 formation at the expense of O_2^- .

Although it may be premature to speculate as to the physiologic significance of our findings, we offer one possible scenario. In the absence of or under low levels of L-arginine, where O_2 reduction is the primary end product of NOS activation, H_4B will undoubtedly play a critical role in regulating the generation of H_2O_2 and O_2^- . Because each of these reduction products of O_2 activates a different cell signal pathway (47, 48), the importance of H_4B in the regulation of NOS-derived O_2^- and H_2O_2 and its diversity of physiological functions cannot be underestimated.

REFERENCES

- Nathan, C., and Xie, Q.-W. (1996) *J. Biol. Chem.* **269**, 13725–13728
- Masters, B. S. S., McMillan, K., Sheta, E. A., Nishimura, J. S., Roman, L. J., and Martasek, P. (1996) *FASEB J.* **10**, 552–558
- Marletta, M. A. (1993) *J. Biol. Chem.* **268**, 12231–12234
- Presta, A., Weber-Main, A. M., Stankovich, M. T., and Stuehr, D. J. (1998) *J. Am. Chem. Soc.* **120**, 9460–9465
- Adak, S., Wang, Q., and Stuehr, D. J. (2000) *J. Biol. Chem.* **275**, 33554–33561
- Klatt, P., Schmidt, K., Lehner, D., Glatter, O., Bächinger, H. P., and Mayer, B. (1995) *EMBO J.* **14**, 3687–3695
- Presta, A., Siddhanta, U., Wu, C., Sennequier, N., Huang, L., Abu-Soud, H. M., Erzurum, S., and Stuehr, D. J. (1998) *Biochemistry* **37**, 298–310
- Reif, A., Fröhlich, L. G., Kotsomis, P., Frey, A., Bömmel, H. M., Wink, D. A., Pfeleiderer, W., and Schmidt, H. H. H. W. (1999) *J. Biol. Chem.* **274**, 24921–24929
- McMillan, K., and Masters, B. S. S. (1993) *Biochemistry* **32**, 9875–9880
- Klatt, P., Schmid, M., Leopold, E., Schmidt, K., Werner, E. R., and Mayer, B. (1994) *J. Biol. Chem.* **269**, 13861–13866
- Nishida, C. R., and Ortiz de Montellano, P. R. (1998) *J. Biol. Chem.* **273**, 5566–5571
- Abu-Soud, H. M., Gachhui, R., Raushel, F. M., and Stuehr, D. J. (1997) *J. Biol. Chem.* **272**, 17349–17353
- Pou, S., Pou, W. S., Bredt, D. S., Snyder, S. H., and Rosen, G. M. (1992) *J. Biol. Chem.* **267**, 24173–24176
- Xia, Y., Roman, L. J., Masters, B. S. S., and Zweier, J. L. (1998) *J. Biol. Chem.* **273**, 22635–22639
- Vásquez-Vivar, J., Kalyanaraman, B., Martásek, P., Hogg, N., Masters, B. S. S., Karoui, H., Tordo, P., and Pritchard, K. A., Jr. (1998) *Proc. Natl. Acad. Sci. U. S. A.* **95**, 9220–9225
- Xia, Y., Tsai, A.-L., Berka, V., and Zweier, J. L., (1998) *J. Biol. Chem.* **273**, 25804–25808
- Pou, S., Keaton, L., Surichamorn, W., and Rosen, G. M. (1999) *J. Biol. Chem.* **274**, 9573–9580
- Vásquez-Vivar, J., Hogg, N., Martásek, P., Karoui, H., Pritchard, K. A., Jr., and Kalyanaraman, B. (1999) *J. Biol. Chem.* **274**, 26736–26742
- Wei, C.-C., Wang, Z.-Q., Wang, Q., Meade, A. L., Hemann, C., Hille, R., and Stuehr, D. J. (2001) *J. Biol. Chem.* **276**, 315–319
- Hurshman, A. R., Krebs, C., Edmondson, D. E., Huynh, B. H., and Marletta, M. A. (1999) *Biochemistry* **38**, 15689–15696
- Gorren, A. C. F., Bec, N., Schrammel, A., Werner, E. R., Lange, R., and Mayer, B. (2000) *Biochemistry* **39**, 11763–11770
- Bec, N., Gorren, A. C. F., Voelker, C., Mayer, B., and Lange, R. (1998) *J. Biol. Chem.* **273**, 9573–9580
- Yoneyama, H., Yamamoto, A., and Kosaka, H. (2001) *Biochem. J.* **360**, 247–253
- Wever, R. M. F., van Dam, T., van Rijn, H. J. M., de Groot, F., and Rabelink, T. J. (1997) *Biochem. Biophys. Res. Commun.* **237**, 340–344
- Nakamura, K., Bindokas, V. P., Kowlessur, D., Elas, M., Milstein, S., Marks, J. D., Halpern, H. J., and Kang, U. J. (2001) *J. Biol. Chem.* **276**, 34402–34407
- Vásquez-Vivar, J., Whitsett, J., Martásek, P., Hogg, N., and Kalyanaraman, B. (2001) *Free Radic. Biol. Med.* **31**, 975–985
- Crane, B. R., Arvai, A. S., Gachhui, R., Wu, C., Ghosh, D. K., Getzoff, E. D., and Stuehr, D. J. (1997) *Science*, **278**, 425–431
- Raman, C. S., Li, H., Martásek, P., Kral, V., Masters, B. S., and Poulos, T. L. (1998) *Cell*, **95**, 939–950
- Zhao, H.; Joseph, J., Zhang, H., Karoui, H., and Kalyanaraman, B. (2001) *Free Radic. Biol. Med.* **31**, 599–606
- Roman, L. J., Sheta, E. A., Martásek, P., Gross, S. S., Liu, Q., and Masters, B. S. S. (1995) *Proc. Natl. Acad. Sci. U. S. A.* **92**, 8428–8432
- Truesdale, G. A., and Downing, A. L. (1954) *Nature*, **173**, 1236
- Kuthan, H., Ullrich, V., and Estabrook, R. (1982) *Biochem. J.* **203**, 551–558
- Asada, K., Takahashi, M., and Nagate, M. (1974) *Agr. Biol. Chem.* **38**, 471–473
- McCord, J. M., and Fridovich, I. (1969) *J. Biol. Chem.* **244**, 6049–6055
- Mohanty, J. G., Jaffe, J. S., Schulman, E. S., and Raible, D. G. (1997) *J. Immunol. Methods* **202**, 133–141
- Zhou, M., Diwu, Z., Panchuk-Voloshina, N., Haugland, R. P. (1997) *Anal. Biochem.* **253**, 162–168

37. Zhou, M., and Panchuk-Voloshina, N. (1997) *Anal. Biochem.* **253**, 169–174
38. Weaver, J., Porasuphatana, S., P. Tsai, Cao, G.-L., Budzichowski, T. A., Roman, L. J., and Rosen, G. M. (2002) *J. Pharmacol. Exp. Ther.* **302**, 781–786
39. Koppenol, W. H., Van Burren, K. J. H., Butler, J., and Braams, R. (1976) *Biochim. Biophys. Acta*, **449**, 157–168
40. Tsai, P., Pou, S., Straus, R., and Rosen, G. M. (1999) *J. Chem. Soc. Perkin Trans. 2*, 1759–1763
41. Finkelstein, E., Rosen, G. M., and Rauckman, E. J. (1980) *J. Am. Chem. Soc.* **102**, 4994–4999
42. Frejaville, C., Karoui, H., Tuccio, B., Le Moigne, F., Culcasi, M., Pietri, S., Lauricella, R., and Tordo, P. (1994) *J. Chem. Soc. Chem. Commun.* 1793–1794
43. Finkelstein, E., Rosen, G. M., Rauckman, E. J., and Paxton, J. (1979) *Mol. Pharmacol.* **16**, 676–685
44. Roubaud, V., Sankarapandi, S., Kuppusamy, P., Tordo, P., and Zweier, J. L. (1997) *Anal. Biochem.* **247**, 404–411
45. Bielski, B. H. J., and Allen, A. O. (1977) *J. Phys. Chem.* **81**, 1048–1050
46. Chance, B. (1952) *Arch. Biochem. Biophys.* **41**, 416–424
47. Finkel, T. (1999) *J. Leukocyte Biol.* **65**, 337–340
48. Konishi, H., Tanaka, M., Takemura, Y., Mataszaki, H., Ono, Y., Kikkawa, U., and Nishizuka, Y (1997) *Proc. Natl. Acad. Sci. U. S. A.* **94**, 11233–11237